Electronic Supplementary Information for

Highly Efficient Catalytic Properties of Sc and Fe Single Atoms Stabilized on Honeycomb Borophene/Al(111) heterostructure via a Dual Charge transfer effect†

Mengru Ren,‡[a] Lili zhang,‡[a] Yandi Zhu,[a] Jinlei Shi,[b] Xingju Zhao,[b] Xiaoyan Ren,*[a] and Shunfang Li*[a]

[a]School of Physics and Microelectronics, Zhengzhou University, Zhengzhou, Henan 450001, China.

[b]Beijing Computational Science Research Center, Beijing 100193, China

This file includes:

Table S1. Interlayer distance (d) and charge transfer (Q) between the h-B cover layer and the Al (111) substrate with and without considering vdW correction.

Table S2. Binding energies Eb of transition metal atoms (TMs) on four high symmetric adsorption sites of h-B/Al(111) substrate.

Fig. S1 (a) Binding energy and **(b)** Charge transfer of TM adatoms on the hollow site of graphene substrate.

Fig. S2 (a) Average binding energy (E_b) of TMn (TM=Sc, Fe; n=1, 2, 3) on h-B/Al(111) calculated by DFT+U (U=3.0 eV). **(b)** The average cohesive energies (ACE) of Sc_N and Fe_N clusters calculated by DFT+U (U=3.0 eV).

Fig. S3 Energy diagrams for **(a)** CO and **(b)** O_2 adsorption on the T_d-Fe_4/h-B/Al(111) complex.

Fig. S4 (a) The most stable configurations and corresponding binding energies (E_b), and **(b)** the diffusion paths and energy barriers (E_{bar}) of Sc and Fe atoms on graphene.

Fig. S5 Temperature (T) fluctuation and the representative snapshots of the geometric structures (both top and side view) of **(a)** Sc/h-B/Al(111), and **(b)** Fe/h-B/Al(111) as a function of the ab initio molecular dynamics simulation time. The time-step is 1 fs.

Fig. S6 L-H reaction process cycle diagram for CO oxidation of SAC-Fe stabilized on h-B/Al (111) substrate.

Fig. S7 Adsorption configuration of O_2 molecules on Fe_1-h-B/Al(111) in relatively high O_2 coverage regime.

Fig. S8 The minimum energy paths for O_2 molecules dissociation on the B atomic sites of the Fe/h-B/Al(111) complexes. In both **(a)** and **(b)**, the O_2 molecules are initially placed more than 3.5 Å above the B cover layer.

Fig. S9 The minimum energy path for CO oxidation by attacking the dissociated O atoms on the B atomic sites of the Fe/h-B/Al(111) complexes.

Fig. S10 L-H reaction process cycle diagram for CO oxidation of SAC-Sc stabilized on h-B/Al(111) substrate.

Fig. S11 The reaction barriers of Sc-SAC and Fe-SAC by plane DFT and DFT+U methods. **(a)** ER mechanism and **(b)** LH mechanism for Sc-SAC; **(c)** ER mechanism and **(d)** LH mechanism for Fe-SAC, respectively.

Fig. S12 Charge transfer (ΔQ) evolution of the key steps presented in the E-R process of CO oxidation on Fe-SAC.

Table S1. Interlayer distance (d) and charge transfer (Q) between the h-B cover layer and the Al (111) substrate with and without considering vdW correction.

|	d	ΔQ
vdW	1.49 Å	0.68 e
Without vdW	1.54 Å	0.68 e

Table S2. Binding energies E_b of transition metal atoms (TMs) on four high symmetric adsorption sites of h-B/Al(111) substrate, i.e., hollow (H), bridge (B), top1 (T1), and top2 (T2).

| E_b(eV)	Sc	Ti	V	Cr	Mn	Fe	Co	Ni	Cu	Pd	Pt	Au	Ag
H	7.48	8.12	7.46	6.44	5.06	5.88	6.16	5.84	4.29	4.58	5.70	3.10	3.02
B	—	—	—	—	—	—	—	—	—	—	—	3.09	—
T1	—	—	—	5.14	3.75	4.19	4.91	4.82	—	4.05	5.32	—	—
T2	—	—	—	5.04	—	4.19	4.84	4.86	—	—	5.52	—	—
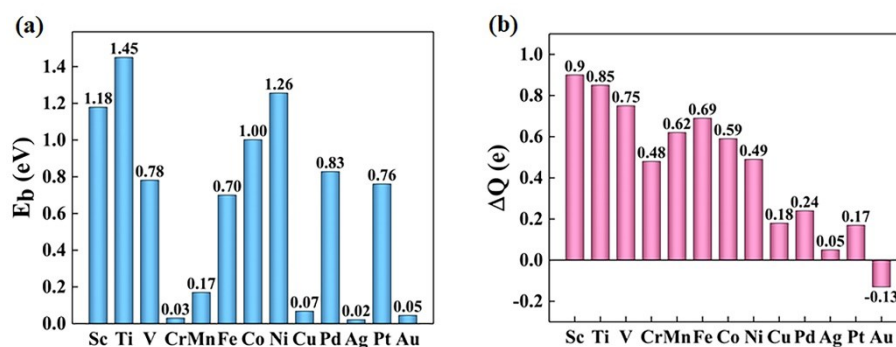
**Fig. S1 (a)** Binding energy and **(b)** Charge transfer of TM adatoms on the hollow site of graphene substrate.
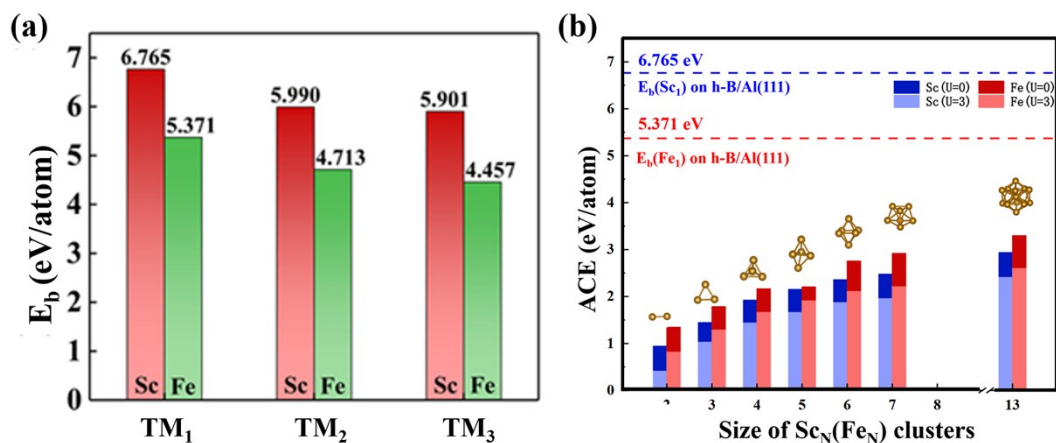
Fig. S2 (a) Average binding energy (E_b) of TM_n (TM=Sc, Fe; n=1, 2, 3) on h-B/Al(111) calculated by DFT+U (U=3.0 eV). **(b)** The average cohesive energies (ACE) of Sc_N and Fe_N clusters calculated by DFT+U (U=3.0 eV).

Here, TM_1, TM_2, and TM_3 represent that the TM_n deposited on the substrate in the forms of single atom, dimer, and trimer, respectively. E_b= [E(TM_n)+E(h-B/Al(111))-E(TM_n/h-B/Al(111))]/n, where the E(TM_n), E(h-B/Al(111)), and E(TM_n/h-B/Al(111)) are the total energies of the TM_n species, the h-B/Al(111) substrate, and the TM_n/h-B/Al(111) complex, respectively. For comparison, the average cohesive energies (ACE) of both Sc_{13} and Fe_{13} are also presented, ACE=-[E(TM_N)-N×E(TM_{atom})]/N, where the E(TM_N) and E(TM_{atom}) are the total energies of the TM_N clusters and TM atom in the gas phase, respectively.
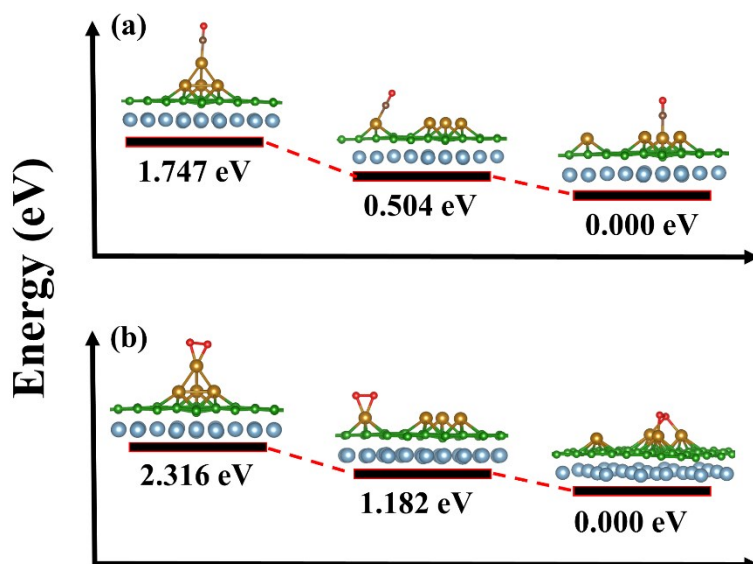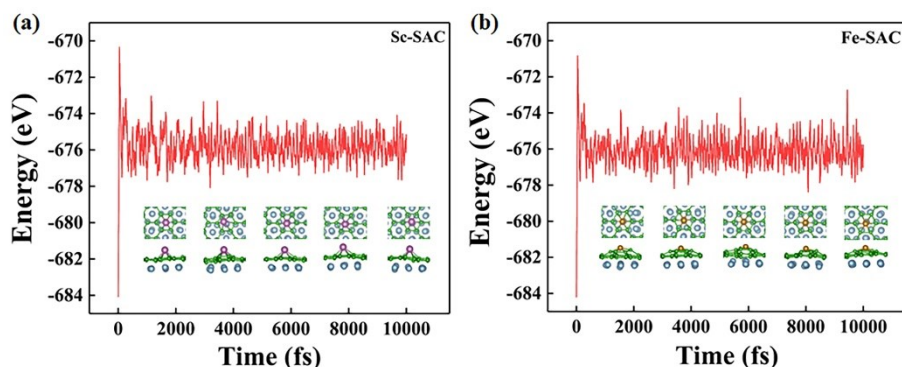

Fig. S3 Energy diagrams for **(a)** CO and **(b)** O_2 adsorption on the T_d-Fe_4/h-B/Al(111) complex.
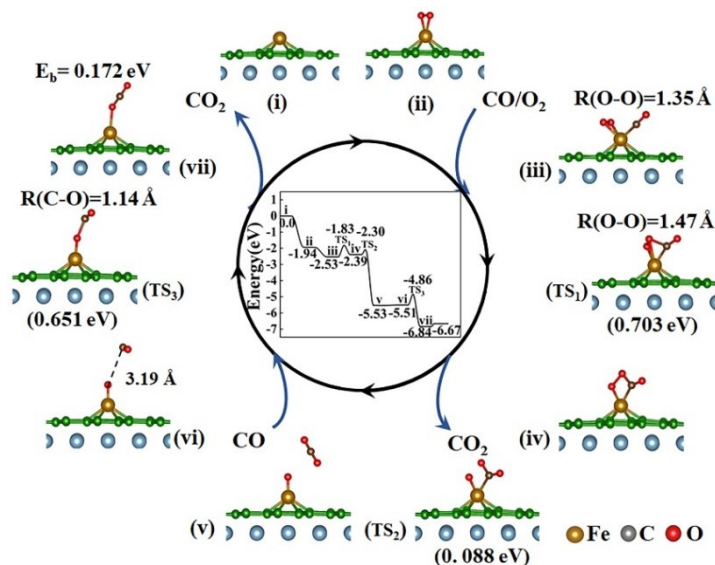
From Fig. S3, one can see that the adsorption of CO and/or O_2 molecule facilitates the dissociation of the T_d-Fe_4 cluster and the generation of the Fe_1 single atoms.
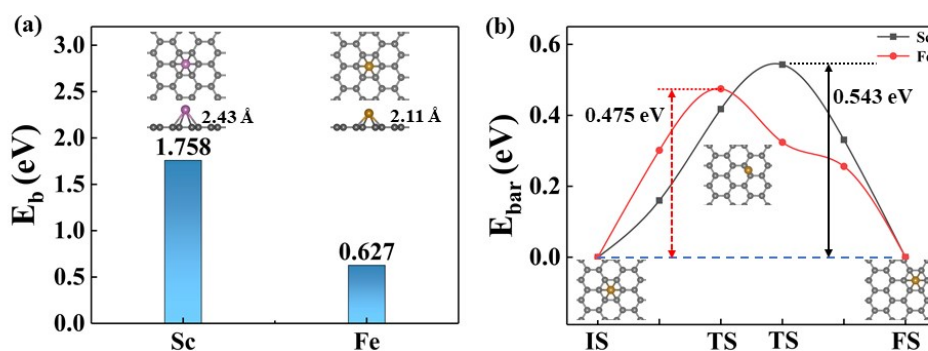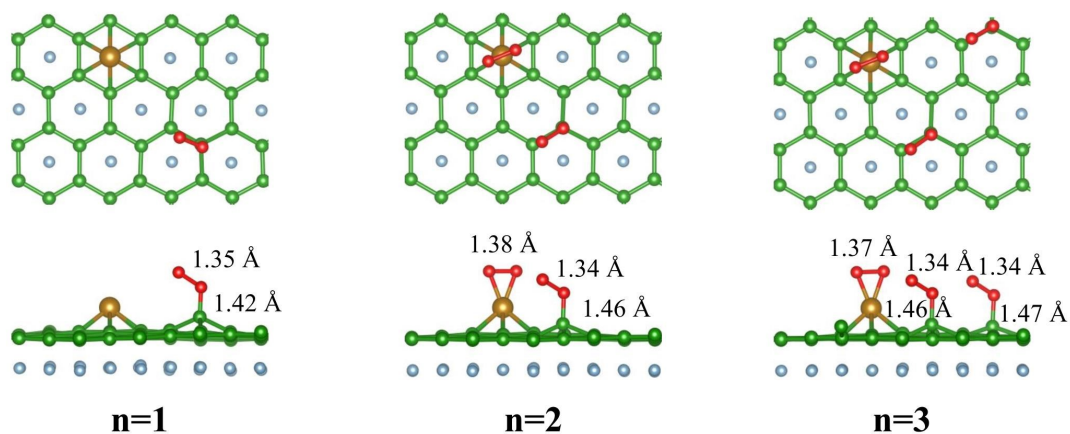
Figure S4. (a) The most stable configurations and corresponding binding energies (E_b), and **(b)** the diffusion paths and energy barriers (E_{bar}) of Sc and Fe atoms on graphene.
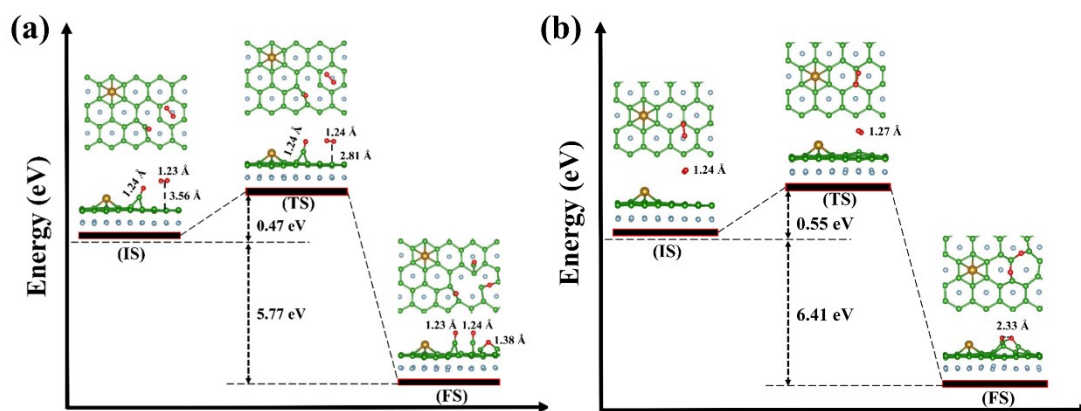

Fig. S5 Temperature (T) fluctuation and the representative snapshots of the geometric structures (both top and side view) of **(a)** Sc/h-B/Al(111), and **(b)** Fe/h-B/Al(111)as a function of the ab initio molecular dynamics simulation time. The time-step is 1 fs.
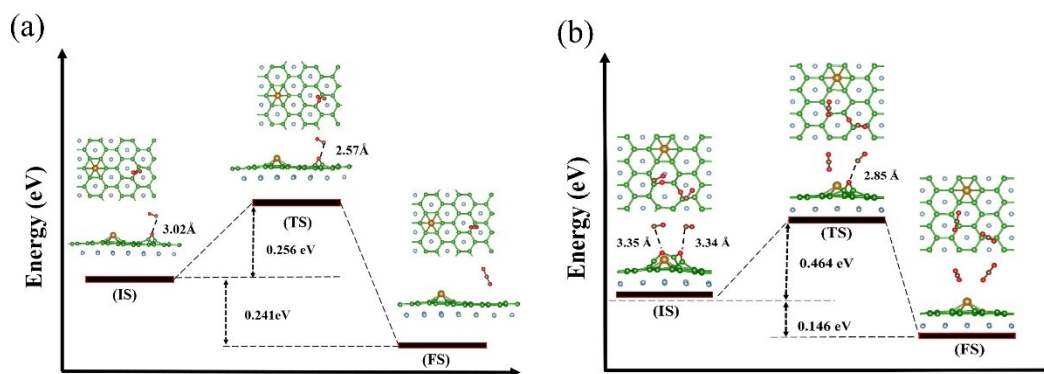

Fig. S6 L-H reaction process cycle diagram for CO oxidation of SAC-Fe stabilized on h-B/Al(111) substrate.

Fig. S7. Adsorption configuration of O_2 molecules on Fe_1-h-B/Al(111) in relatively high O_2 coverage regime.


Fig. S8 The minimum energy paths for O_2 molecules dissociation on the B atomic sites of the Fe/h-B/Al(111) complexes. In both **(a)** and **(b)**, the O_2 molecules are initially placed more than 3.5 Å above the B cover layer.
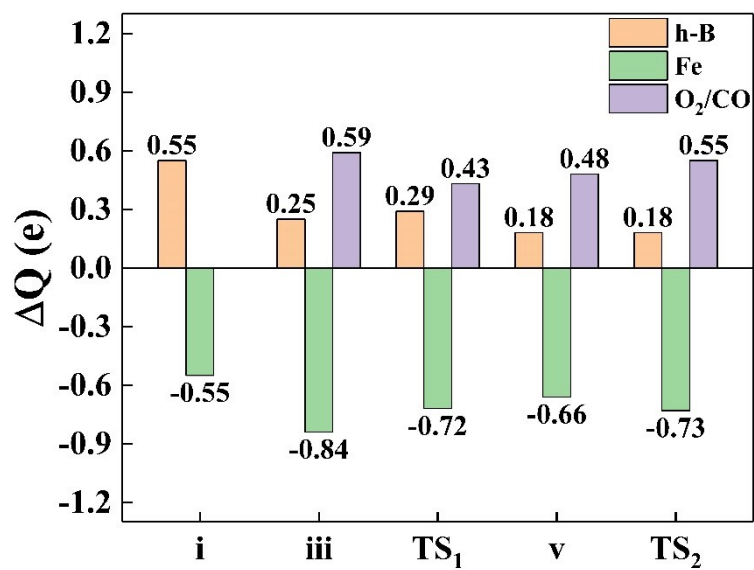

Fig. S9 The minimum energy paths for CO oxidation by attacking the dissociated O atoms on the B atomic sites of the Fe/h-B/Al(111) complexes. **(a)** one CO molecule attacking one O atom, **(b)** two CO molecules attacking two dissociated O atoms.
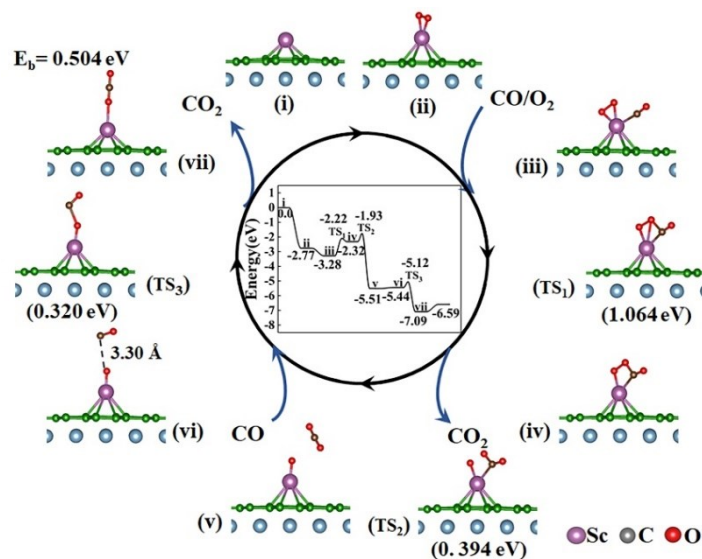
Fig. S10 L-H reaction process cycle diagram for CO oxidation of SAC-Sc stabilized on h-B/Al(111) substrate.
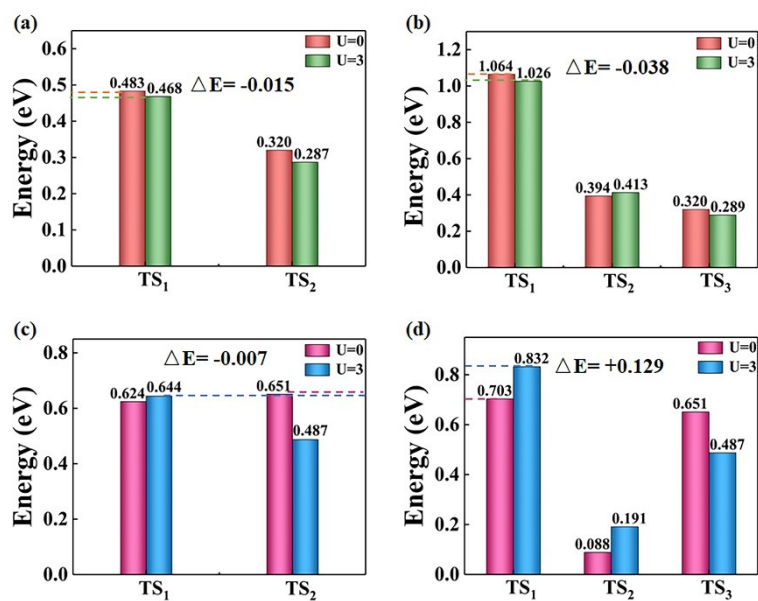
Fig. S11 The reaction barriers of Sc-SAC and Fe-SAC by DFT and DFT+U methods. **(a)** ER mechanism and **(b)** LH mechanism for Sc-SAC; **(c)** ER mechanism and **(d)** LH mechanism for Fe-SAC, respectively.

Fig. S12 Charge transfer (ΔQ) evolution of the key steps presented in the E-R process of CO oxidation on Fe-SAC.